In-situ development of self-defensive antibacterial biomaterials: phenol-g-keratin-EC based bio-composites with characteristics for biomedical applications

Dr Hafiz Iqbal[1]
Dr Godfrey Kyazze[1]
Dr Ian Locke[1]
Thierry Tron[2]
Prof Taj Keshavarz[1]

[1] Faculty of Science and Technology, University of Westminster, London, UK
[2] Aix Marseille Université, CNRS, Marseille, France

Green Chemistry

Dynamic Article Links ►

Cite this: DOI: 10.1039/c0xx00000x

www.rsc.org/xxxxxx

PAPER

In-situ development of self-defensive antibacterial biomaterials: phenol-*g*-keratin-EC based bio-composites with characteristics for biomedical applications

Hafiz M. N. Iqbal*[a] Godfrey Kyazze[a] Ian Charles Locke[a] Thierry Tron[b] and Tajalli Keshavarz*[a]

Received (in XXX, XXX) Xth XXXXXXXXX 20XX, Accepted Xth XXXXXXXXX 20XX
DOI: 10.1039/b000000x

Recently, the development of highly inspired biomaterials with multi-functional characteristics has gained considerable attention, especially in biomedical, and other health-related areas of the modern world. It is well-known that the lack of antibacterial potential has significantly limited biomaterials for many challenging applications such as infection free wound healing and/or tissue engineering *etc*. In this perspective, herein, a series of novel bio-composites with natural phenols as functional entities and keratin-EC as a base material were synthesised by laccase-assisted grafting. Subsequently, the resulting composites were removed from their respective casting surfaces, critically evaluated for their antibacterial and biocompatibility features and information is also given on their soil burial degradation profile. *In-situ* synthesised phenol-*g*-keratin-EC bio-composites possess strong anti-bacterial activity against Gram-positive and Gram-negative bacterial strains *i.e., B. subtilis* NCTC 3610, *P. aeruginosa* NCTC 10662, *E. coli* NTCT 10418 and *S. aureus* NCTC 6571. More specifically, 10HBA-*g*-keratin-EC and 20T-*g*-keratin-EC composites were 100% resistant to colonisation against all of the aforementioned bacterial strains, whereas, 15CA-*g*-keratin-EC and 15GA-*g*-keratin-EC showed almost negligible colonisation up to a variable extent. Moreover, at various phenolic concentrations used, the newly synthesised composites remained cytocompatible with human keratinocyte-like HaCaT, as an obvious cell ingrowth tendency was observed and indicated by the neutral red dye uptake assay. From the degradation point of view, an increase in the degradation rate was recorded during their soil burial analyses. Our investigations could encourage greater utilisation of natural materials to develop bio-composites with novel and sophisticated characteristics for potential applications.

Introduction

Since the late 1990s, enzyme-based techniques have evolved from the biotransformation of natural and synthetic materials into value-added products. A new global thrust towards green chemistry and recent advancement in polymer synthesis and/or modifications via grafting is gaining higher interests due to the accrued understanding of enzyme reaction mechanisms.[1-5] Moreover, enzyme as green catalyst in polymeric-based materials synthesis and modifications offer a potential of eliminating the hazards associated with other chemical-based procedures.[6-8] Recently, microbial laccase has gained particular interests owing to its versatile bio-catalytic potential to oxidise a wider range of substrates such as phenols, diamines, benzenethiols, polyphenols, organic/inorganic compounds and many others, however, it does not require any additional initiators e.g., H_2O_2.[3, 9] Owing to the tremendous phenoxy radicals generation capability of laccases, thereby enhancing the reactivity of polymers and forms the basis of their application in polymer chemistry.[10] The laccase-generated radicals provide ideal sites for cross-linking of various molecules of interests leading to grafting and/or formation of new biomaterials with novel characteristics.

Because of increasing consciousness and demands to reduce bacterial contaminations in healthcare facilities and possibly to cut pathogenic infections, development of novel anti-microbial active materials are considered to be a potential solution to such a problematic issue. In past years, several authors have already been reported antibacterial features of silver nanoparticles.[11-13] However, excess release of silver nanoparticles inhibits osteoblasts growth and can also cause many severe side effects such as cytotoxicity.[13] Therefore, there is a persistent need to prepare green composites using one or more individual bio-polymers to reduce or even eliminate the risk of bacterial infection without impairing the cytotoxicity capabilities.

The antibacterial potential of natural phenols, along with their flavouring, antioxidant, and antiseptic characteristics, has already been reported elsewhere.[14-16] Research on several proteins, including collagen, fibroin, keratin, and others is in progress for the development of materials with multifunctional characteristics. Among the natural materials, keratinous proteins are interesting

candidates to prepare keratin-based composites which in turn may find potential applications in bio-medical, pharmaceutical, tissue engineering, and cosmetic industries.[17] On the basis of these evidences, we hypothesised that natural phenols are the most efficient choice for inhibiting bacterial infections and investigated the antibacterial features of these compounds, incorporated in/on keratin-EC based materials. Figure 1 illustrates a schematic mechanism of laccase-assisted grafting of natural phenols onto the keratin-EC based composite.

Please insert Fig. 1 here

Figure 1 A schematic representation of proposed mechanism of graft formation; (**A**) between keratin and EC, (**B**) between keratin-EC and caffeic acid, (**C**) between keratin-EC and gallic acid, (**D**) between keratin-EC and *p*-4-hydroxybenzoic acid, and (**E**) between keratin-EC and thymol.

Grafting is preferred over other physiochemical techniques in order to obtain the requisite properties which individual materials fail to demonstrate on their own. Effective modifications should include changes in chemical group functionality, surface charge, biocompatibility and biodegradability.[2, 3] The aforementioned both biopolymers *i.e.*, keratin and EC are among excellent candidate biomaterials with outstanding properties that make them valuable especially in the field of biomedical and other areas of biomaterial based sectors.[18] Thus, a notable amount of information on the characteristics and hydrolysis of keratin has become available where recalcitrant keratinous waste are converted into valuable products.[17-20]

To date, our laboratory has developed a number of novel bio-composites.[2-5] Nowadays, biopolymers are playing critical roles in many applications where the materials are in direct contact with body tissue, *e.g.*, skin or wound healing. Despite the increasing number of reports on using bio-tools for tuning materials properties using laccase to graft the aforementioned natural phenols onto the keratin-EC based bio-composites, aiming at infection free wound healing application has not been reported yet. Therefore, in this study, a series of bio-composites were synthesised through laccase-assisted grafting of natural phenols onto the keratin-EC. The newly synthesised bio-composites were critically evaluated for their antibacterial, biocompatibility and biodegradability features to propose their potential application, particularly in the area of infection free wound healing.

Experimental section

Chemicals/reagents/materials

A fungal laccase from *Trametes versicolor* with a unit activity ≥ 10 U/mg was obtained from Sigma-Aldrich Company Ltd., UK and used as-received to prepare keratin-EC, and phenol grafted keratin-EC bio-composites. Dulbecco's modified eagle's medium (DMEM), phosphate buffer saline (PBS), streptomycin and penicillin were obtained from Lonza, Wilford Industrial Estate, Nottingham, UK. Fetal calf serum was obtained from Labtech International Ltd., Bellbrook Industrial Estate, East Sussex, UK. Phenolic compounds *i.e.*, caffeic acid (CA), gallic acid (GA), *p*-4-hydroxybenzoic acid (HBA), and thymol (T) were purchased from Sigma-Aldrich Company Ltd., UK (Table S1). All other chemicals and/or reagents used in this study were of analytical laboratory grade and used as-received.

Microbial cultures and maintenance

Gram-positive (*Bacillus subtilis* NCTC 3610 and *Staphylococcus aureus* NCTC 6571) and the Gram-negative (*Escherichia coli* NTCT 10418 and *Pseudomonas aeruginosa* NCTC 10662) strains were obtained from the culture collection unit of the University of Westminster London, UK. In order to obtain single bacterial colonies, each of the collected bacterial strains was sub-cultured, using streak plate method on sterile nutrient agar plates under sterilised environment. Following that a single pure colony from each of the aforementioned strains was grown in 50 mL sterile nutrient broth under temperature controlled environment for 24 h at 30 °C and 120 rpm. The initial bacterial concentration was maintained approximately at 1×10^5 CFU/mL by comparing OD_{600} via 0.5 McFarland standard method.

Grafting of natural phenols onto keratin-EC

Prior to grafting, phenolic solutions of CA, GA, HBA, and T, with different mM concentrations ranging from 5 to 20 were prepared. Subsequently the surface dipping and incorporation (SDI) technique was adopted to graft the aforementioned phenolic agents onto the keratin-EC based composite. Briefly, previously extracted keratin from chicken feathers and ethyl cellulose (EC) were used to prepare baseline composite *i.e.*, keratin-EC using as-reported laccase-assisted grafting.[5] Finally, each of the pre-weight (keratin-EC) composites were dipped in a glass basin containing 50 mL of pre-dissolved CA, GA, HBA and T, separately, in the presence of laccase for 60 min of reaction time at 30 ^oC under constant stirring at 100 rpm. Control samples were also treated in the same way using sodium malonate buffer alone without adding any of the aforementioned natural phenol. After the stipulated reaction time, the weight of each composite was recorded in the swollen state followed by incubation at 50 ^oC until fully dried. Afterwards all of the composites were washed three times with sodium malonate buffer to eliminate any of the un-reacted phenolic contents, and then dried again at 50 ^oC and final dry weight after immersion was recorded to calculate the grafting parameters. All of the samples were prepared in triplicates. The newly synthesised bio-composites were assigned IDs subject to the concentration of the phenol used, as shown in Table 1.

Table 1 Designation of IDs to the newly synthesised phenol grafted keratin-EC bio-composites subject to the concentration of phenol used for grafting purposes.

Please insert Table 1 here

Evaluation of structural elements (FT-IR)

FT-IR spectroscopy was used primarily to identify the structural elements of the individual phenols, keratin-EC and their respective grafted composites. Each of the grafted composites and their individual counterparts were placed directly on the diamond crystal, and infrared absorption spectra were recorded

from the wavelength region of 4000-500 cm^{-1} using a Perkin Elmer System 2000 FT-IR spectrophotometer. All spectra were collected with 64 scans and 2 cm^{-1} resolution and assigned with peak numbers.

Evaluation of grafting parameters

The effect of different phenolic concentrations used in the grafting process between CA, GA, HBA, and T and keratin-EC base material was investigated in terms of grafting parameters *i.e.,* graft yield (GY %), grafting efficiency (GE %) and swelling ratio (SR %). The grafting parameters were calculated according to the following equations.

Graft yield (GY%) = [(Wf – Wi) / Wi] X 100 (1)

Grafting efficiency (GE%) = [(Wf – Wi) / (Ws – Wi)] X 100 (2)

Swelling ratio (SR%) = Ws − Wi / Wi × 100 (3)

Where, Wi = initial weight before immersion; Wf = final dry weight after immersion; and Ws = weight of sample at the swollen state

Evaluation of antibacterial activity

The antibacterial characteristics of the newly synthesised bio-composites were tested against *B. subtilis* NCTC 3610, *S. aureus* NCTC 6571, *E. coli* NTCT 10418 and *P. aeruginosa* NCTC 10662. Prior to culture, an overnight grown spore suspensions (containing approximately 1×10^5 CFU/mL) onto the surfaces of the test composites, all of the composites were thermally sterile at 90 ^oC for 30 min. The inoculated test composites were placed onto the sterile moisture pads followed by incubation in a temperature controlled incubator at 30 °C for 24 h. After the stipulated incubation time (24 h), the bacterial cells from the control and test composites were washed twice using 50 mL phosphate buffer (pH, 7.0). The viable cell number in each of the washed suspension was determined by conventional spread-plate method and plate counter agar was used to calculate the CFU/mL by serial dilution. The g/L constituents of the plate counter agar were as: tryptone, 5; yeast extract, 2.5; glucose, 1 and agar, 9. After 24 h incubation on plate counter agar medium at 30 ^oC, the replicates were examined and the results were expressed as mean colony forming units per mL (CFU/mL). In comparison with the control (initial bacterial count *i.e.,* 1×10^5 CFU/mL) the CFU/mL values were used to calculate the antibacterial efficacy of the test specimens by using the following equation:

Log reduction = log CFU control sample − log CFU treated sample (4)

A 2 log reduction was considered necessary to claim an antibacterial activity.

***In-vitro* biocompatibility evaluation**

A sterilised DMEM additionally supplemented with 10% fetal calf serum, 100 mg/mL streptomycin and penicillin was used to culture Human keratinocytes-like (HaCaT) skin cell line. The inoculated culture was incubated at 37 ^oC in a humidified atmosphere of 5% CO_2. After 24 h of initial incubation, the confluent cells were subjected to trypsinisation and recovered by centrifugation at 1000 *g* for 10 min. The cell pellets were re-suspended homogenously into the culture media and then transferred into a 75 cm^2 tissue culture flask for further passages.

***In-vitro* cell viability assay**

HaCaT cells were adopted to evaluate the biocompatibility of the newly synthesised bio-composites, and the cell viability was determined using neutral red assay, as described elsewhere.[20] Prior to *in-vitro* testing, the test composites (1 cm^2 in area) were sterilised using UV radiation for 30 min on each side and placed in a 24-well tissue culture plates. After cell counting, HaCaT cells were seeded in 24-well tissue culture plates containing test composites at a density of 1×10^5 cells per well. After incubating for 1, 3 and 5 days respectively, DMEM were removed and the test composites were rinsed three times using phosphate buffer saline in order to remove the non-adhered HaCaT cells. Cell viability of the adherent cells was measured by adding 1 mL/well culture medium containing neutral red dye and incubated for 3 h to allow the viable cells to uptake the dye. After 3 h incubation, the test composites were again washed with a mixture solution containing 1% $CaCl_2$ and 0.5% formaldehyde. This was followed by 10 min incubation in lysate solution to extract the dye taken up by the viable cells. Then 100 µL from each well was transferred to new 96-well cell culture plates and optical density (OD value) of the extracted supernatant was measured with a Thermomax micro-plate reader (Model 680, Bio-Rad, CA) at 540 nm. The percent viability was calculated using the following equation:

$$\% \text{ cell viability} = \frac{OD_{\text{Test specimen}} - OD_{\text{Negative control}}}{OD_{\text{Positive control}}} \text{ X } 100 \quad (5)$$

In this experiment, standard tissue culture plastic was used as a positive control whereas graft composite without cell culture was used as negative control to normalise the absorption of the neutral red dye by the graft composite itself.

Adherent Morphology

The adherent morphology of HaCaT cell line seeded on the test composites was observed using Nikon light microscope. After 1, 3 and 5 days of incubation at 37 ^oC in a humidified atmosphere of 5% CO_2 cells were washed with PBS and then fixed with 4% (w/v) paraformaldehyde in PBS for 30 min followed by adding 5 mg/mL neutral red dye to stain HaCaT cells for 1 h. Afterwards, the stained cells were washed three times with PBS for 15 min and the stained signals in the cells were recorded by taking high definition images (HDI) using DCMI-15 Nikon light microscope camera.

Evaluation of soil burial degradation

To determine the bio-degradability of the newly synthesised composites as reported method,[21] with some minute alternations was adopted, in this study. Briefly, test specimens about 30×30×1 mm in sizes were cut from each of the composite, dried and equilibrated at room temperature in desiccators, and weighed to determine the reference weight (control). The soil burial test lasted for 6 weeks (42 days). A garden type soil was placed into plastic containers (pots) with 25 cm in diameter and 20 cm in height with tiny holes perforated at the bottom and on the sides of the containers to increase air and water circulation to promote the microbial action of the microorganisms which are normally present in the soil. A set of triplicate composites were buried under the soil surface of approximately 8-10 cm. After every 7 days of burial, each set was removed, washed with distilled water, dried under an ambient environment (30 °C) and

subsequently weighed to determine the loss in weight, being recorded every week for 6 weeks. The percentage weight loss was calculated using the following equation.

$$\% \text{ Loss in weight} = \frac{\text{Control weight} - \text{loss in weight}}{\text{Control weight}} \times 100 \quad (6)$$

Statistical analysis

In the present study, all of the quantitative data analyses were conducted in triplicate (n=3). The data collected was subjected to the analysis of variance (ANOVA) using Windows based version MINITAB15 software and P-value ($p \leq 0.01$) was considered significant. The statistically evaluated results are presented as mean ± S.E. of means and S.E values are displayed in figures as Y-error bars.

Results and Discussion

Evaluation of structural elements (FT-IR)

Infrared absorption spectra of CA, GA, HBA, T, CA-*g*-keratin-EC, GA-*g*-keratin-EC, HBA-*g*-keratin-EC and T-*g*-keratin-EC composites show characteristic absorption bands assigned to the peptide bonds (-CONH-) that originate bands known as amide I, amide II, and amide III (Fig. 2 A-D). In IR spectral analysis, amide I is mainly related with the C=O stretching, and it occurs in the range of 1,700-1,600 cm^{-1}, whereas, amide II is mainly related to the N-H bending and C-H stretching vibration, and it occurs in the range of 1,540-1,520 cm^{-1}. Finally, amide III is mainly originated from in-phase combination of C-N stretching and C=O bending vibration, and it occurs in the range of 1,220-1,300 cm^{-1}.[18, 22] Moreover, as can be seen form the Figure 2, the positions of the aforementioned bands indicate the conformations of the grafted materials: 1,630 cm^{-1} for amide I, and 1,270 cm^{-1} for amide III.[22, 23] Evidently, a typical peak at 1,056 cm^{-1} region was observed with a sharp appearance which is due to the C–O–C stretching and specifically linked to the cellulose molecules.[3] The peaks present near to the 2,930 and 2,850 cm^{-1} are characteristic infrared bands of aliphatic hydrocarbons of methylene asymmetric C–H stretching and symmetric C–H stretching, respectively. However, both signals for the methyl (CH_3) asymmetric and symmetric modes and the methylene (CH_2) asymmetric and symmetric modes originated from keratin and can be assigned to the aliphatic chain. In comparison to the pristine CA and HBA, a broad peak appeared in the spectra of CA-*g*-keratin-EC and HBA-*g*-keratin-EC at 3,345 cm^{-1} region which typically corresponds to the phenolic -OH stretching and the involvement of hydrogen bonding type interactions between those -OH groups.[14] On the other hand, GA-*g*-keratin-EC and T-*g*-keratin-EC composites have typical polyphenol characteristics, showing broad peaks cantered at 3,360 cm^{-1} which are due to the vibrational mode of -OH linkage of phenolic and hydroxyl groups. The higher wavenumber of amide I can be explained by the protein extraction procedure suggesting again the presence of R-helix structure. Nevertheless, an increase in the peak area of the amide I band in the grafted composites spectra with respect to the same band in the individual counterparts spectra indicates the stabilisation of R-helix conformation and destabilisation and/or the involvement of the *β*-sheet structure during the graft formation process.

Please insert Fig. 2 here

Figure 2 Typical FT-IR spectra: (A) CA, keratin-EC and CA-*g*-keratin-EC, (B) GA, keratin-EC and GA-*g*-keratin-EC, (C) HBA, keratin-EC and HBA-*g*-keratin-EC and (D) T, keratin-EC and T-*g*-keratin-EC bio-composites.

Evaluation of grafting parameters

To evaluate the grafting behaviour, following parameters were investigated to record the graft yield (GY %), grafting efficiency (GE %) and swelling ratio (SR %) profiles of the newly synthesised bio-composites. The data revealed that the ultimate graft yield, grafting efficiency and swelling ratio values were maximum in case of 15CA-g-keratin-EC (Figure 3A). One possible reason for the observed behaviour could be the substantial amount of CA grafted onto the baseline (keratin-EC) composite, which creates steric hindrance for further grafting on increasing beyond the optimal point. The results of the grafting parameters of GA-*g*-keratin-EC as a function of GA are shown in Figure 3B. In comparison to the control sample a consistent increase in the swelling ratio in addition to the graft yield and grafting efficiency was recorded, where, 15GA-*g*-keratin-EC was proved best under the same environment. In Figure 3C, the grafting profile of the HBA-*g*-keratin-EC is shown. The grafting between HBA and keratin-EC was maximum when the composite was prepared using 10 mM HBA followed by 15 mM HBA under the same reaction conditions and the difference between the grafting behaviour was insignificant in both of the composites *i.e.*, 10HBA-*g*-keratin-EC and 15HBA-*g*-keratin-EC. However, in comparison to the other two composites *i.e.*, 5HBA-*g*-keratin-EC and 20HBA-*g*-keratin-EC the grafting behaviour was much higher and significant in 10HBA-*g*-keratin-EC and 15HBA-*g*-keratin-EC. The grafting parameter's profile of the composites prepared using T as a functional entity is shown in the Figure 3D. Indeed, the profile presented in Fig. 3D indicates a gradual increase in the GP% as the concentration of T increases from 0 to 20 mM. One possible reason for behaviour could be the availability of lower no of functional groups, hence more active sites were available in the baseline keratin-EC to accommodate higher ratio of T as compare to other tested phenols. The cross-linking of a polymer greatly influence its affinity by imparting rigidity in the long chain macromolecules, and, therefore, polymeric networks swell when they are exposed to an aqueous phase of the reaction process. It has also been reported in literature that the degree of swelling and/or swelling ratio is a function of several factors of which the length of the polymeric network chain is the prime one,[24] whereas other includes the molecular weight and the cross-links. Even though the backbone material used herein, keratin-EC is highly structured and bulky, swelling of the backbone may take place which enhance the mobility of radicals generated (*e.g.* in our case by laccase) to active sites on the backbone to effect grafting. The presence of functional groups in the backbone material (keratin-EC) also influences the grafting behaviours in terms of graft yield and grafting efficiency. It is often reported and as observed here in this study, the grafting efficiency increases with monomer concentration up to a certain limit and then decreases with further

increase in the concentration.[24, 25] This behaviour may reflect an initial increase of the monomer concentration in close proximity to the backbone material (keratin-EC). Analysis of variance of the data (Tables S2 to S5) showed a significant difference ($p \leq 0.01$) between grafting parameters *i.e.*, graft yield, grafting efficiency and swelling ratio behaviours of CA, GA, HBA, T, keratin-EC, CA-*g*-keratin-EC, GA-*g*-keratin-EC, HBA-*g*-keratin-EC and T-*g*-keratin-EC bio-composites.

Please insert Fig. 3 here

Figure 3 Evaluation of grafting parameters *i.e.*, graft yield, grafting efficiency and swelling ratio behaviours of CA, keratin-EC and CA-*g*-keratin-EC (A), GA, keratin-EC and GA-*g*-keratin-EC (B), HBA, keratin-EC and HBA-*g*-keratin-EC (C) and T, keratin-EC and T-*g*-keratin-EC (D).

Evaluation of antibacterial activity

Figure 4 reports the anti-bacterial activities of CA-*g*-keratin-EC, GA-*g*-keratin-EC, HBA-*g*-keratin-EC and T-*g*-keratin-EC against *B. subtilis* NCTC 3610, *S. aureus* NCTC 6571, *E. coli* NTCT 10418 and *P. aeruginosa* NCTC 10662 strains. Evidently, different anti-bacterial behaviour is observed for the composites prepared with different mM concentrations of CA: 15CA-*g*-keratin-EC showed excellent bactericidal and bacteriostatic potential against *E. coli* NTCT 10418 and *P. aeruginosa* NCTC 10662 and *B. subtilis* NCTC 3610 and *S. aureus* NCTC 6571 strains, slightly more than 10CA-*g*-keratin-EC, which only showed bacteriostatic activity against Gram-negative strains. Whereas, 5CA-*g*-keratin-EC and 20CA-*g*-keratin-EC showed negligible reduction in the bacterial count verses all of the tested strains. As compare to the keratin-EC, 15GA-*g*-keratin-EC showed more prominent resistive properties (complete killing of bacteria) against *E. coli* NTCT 10418 and *P. aeruginosa* NCTC 10662. This was followed by 10GA-*g*-keratin-EC which was slightly higher against *E. coli* NTCT 10418 and *P. aeruginosa* NCTC 10662 than *B. subtilis* NCTC 3610 and *S. aureus* NCTC 6571. However, 5GA-*g*-keratin-EC only showed bacteriostatic potential against Gram-negative strains, whereas, *B. subtilis* NCTC 3610 was found able to withstand against the lower concentration of GA used.

An excellent level of anti-bacterial properties of HBA-*g*-keratin-EC was observed against the test bacterial species. In case of 10HBA-*g*-keratin-EC, a maximum of five log reductions (100% bactericidal) was observed as compared to the pristine keratin-EC. In case of 15HBA-*g*-keratin-EC, the log value decreased from 5 to 0 and 1 against *E. coli* NTCT 10418 and *P. aeruginosa* NCTC 10662 and *B. subtilis* NCTC 3610 and *S. aureus* NCTC 6571 strains, respectively. Among others, only 5HBA-*g*-keratin-EC showed slight bacteriostatic activity whereas, the remaining bacterial count was negligible in case of 20HBA-*g*-keratin-EC. The levels of anti-bacterial activity observed were maximum with 20T-*g*-keratin-EC and 15T-*g*-keratin-EC with a greater than 4 log reductions. Although there was less reduction in the bacterial count with 10T-*g*-keratin-EC but the level was still well above the minimum acceptable anti-bacterial (bacteriostatic) activity level of 2 and it was particularly against the *E. coli* NTCT 10418 and *P. aeruginosa* NCTC 10662. The anti-bacterial mechanism of natural phenols is naturally concomitant due to the presence of active hydroxyl groups. This is because the interaction between natural phenols and bacteria can change the metabolic activity of bacteria and eventually cause their death. Based on an earlier published data, most of the phenolic compounds including those used in this study have an ability to disrupt the lipid structure of the bacterial cell wall, further leading to a destruction of the cell membrane, cytoplasmic leakage, and cell lysis which ultimately leads towards the cell death.[15, 26, 27] It is well-known that the anti-bacterial mechanism of phenols, such as CA, GA, HBA and T, is natural which is due to the availability of reactive acidic hydroxyl groups. Furthermore, the delocalisation of the electrons on their structure has also been reported to contribute to their activity as well.[16, 28] Based on the optimal grafting and antibacterial activities, the best yielded composites were selected to investigate for HaCaT biocompatibility and biodegradability analyses.

Please insert Fig. 4 here

Figure 4 Evaluation of antimicrobial potential of CA-*g*-keratin-EC (A), GA-*g*-keratin-EC (B), HBA-*g*-keratin-EC (C) and T-*g*-keratin-EC (D) against *B. subtilis* NCTC 3610 (⬚); *S. aureus NCTC* 6571 (▩); *E. coli NTCT* 10418 (▨) and *P. aeruginosa NCTC* 10662 (▩). Red line indicates an initial bacterial count *i.e.*, 1×10^5 CFU/mL. An increase in this count (as compared to the initial bacterial count) showed susceptibility whereas, reduction in the initial bacterial count showed bacteriostatic and bactericidal activities of the respective composites. A 2 log reduction was considered to claim an antibacterial activity.

***In-vitro* biocompatibility evaluation**

In this study, HaCaT cell line viability on the UV sterilised surfaces of the newly synthesised bio-composites *i.e.*, 15CA-*g*-keratin-EC, 15GA-*g*-keratin-EC, 10HBA-*g*-keratin-EC and 20T-*g*-keratin-EC was investigated, i*n-vitro*. The % viability and adherent morphology of HaCaT cells on as-prepared and selected composites was determined quantitatively using neutral red assay and staining procedures, respectively. The percent viability was recorded against each sample seeded for 1, 3 and 5 days in 24-well tissue culture plates containing test composites at a density of 1×10^5 cells per well using culture media (DMEM). Notably, all of the aforementioned composites displayed up to 100% cell viability after 5 days of incubation (Figure 5), indicating that the test composites were non-cytotoxic in nature thus promote the viability of HaCaT cells. However, the growth rate after 1 and 3 days of incubation was found variable which could be due to the sudden change in the environment or may because of the nature of each phenolic component used. However, after incubating for 5 days the viability rate revealed no differences among all test composites, because the cells became saturated on the surface of the composites, and no cytotoxicity was observed in all of the test specimens. A morphological overview of the HaCaT cells is shown in Fig. 6. With the extension of culture time from day 1 to day 5 the number of cells attached to the seeded composite surfaces was increased. It could be seen from Fig. 6, the HaCaT cells adhered on the composites, and spread in a stretchy way on their surfaces. Furthermore, after long-term culture (5 days), it

was found that no significant difference could be found among all of the test composites, and HaCaT cells covered almost the whole surfaces at 5 days of incubation. Statistical analysis of data by ANOVA revealed significant difference ($p \leq 0.01$), when compared all the treatments were found to have significant differences (Table S6).

Please insert Fig. 5 here

Figure 5 Neutral red dye concentration dependent percentage cell viability of HaCaT cells seeded on the selected bio-composites for prescribed periods (n = 3).

Please insert Fig. 6 here

Figure 6 Adherent morphology of the stained images of HaCaT cells seeded on the selected bio-composites (15CA-*g*-keratin-EC, 15GA-*g*-keratin-EC, 10HBA-*g*-keratin-EC and 20T-*g*-keratin-EC) surfaces for prescribed periods (1, 3 and 5 Days). All images were taken at 100× magnification.

Evaluation of soil burial degradation

The effect of the soil burial degradation, as observable by the weight loss of the pristine backbone and phenol grafted keratin-EC bio-composites buried for prescribed periods, is reported in Figure 7. The percent weight loss of the grafted composites was significantly affected by their formulation using different phenols, while a negligible difference was observed from day 7 to day 21 of degradation. In particular, the weight loss increased from 23 ± 0.9% to 29 ± 1.1% for the keratin-EC composite, this difference remaining almost constant in all of the tested composites up to day 21 (Figure 7 A-C). Statistical analysis of the degradability data by ANOVA revealed a significant difference ($p \leq 0.01$) within the treatments (Table S7), subject to the specified burial period. The observed degradation behaviour is directly dependent on the multi-phase and portentous nature of the composites which is due to the presence of keratin in them. Notably, after increasing the burial period from 21 days to 42 days, an increase in the weight loss from 43 ± 2.2% to 99 ± 3.5% was recorded for the keratin-EC composite (Figure 7 C-F). On the other hand, in case of phenol grafted keratin-EC bio-composites, a 100% degradation was observed after 42 days of controlled incubation. Whereas, the degrading behaviour was least in 20T-*g*-keratin-EC with an overall weight loss of 85 ± 2.2% (Figure 7 F). This behaviour can be well explained taking into account the results of the swelling ratio from the grafting parameters test that have demonstrated the high swelling linked to the water absorption capacity of the composites. Therefore, it seems evident that the swelling capability linked to the water absorption capacity plays a crucial role by causing the hydrolysis of surfaces and interfaces to determine the degradation kinetics of the composites.[29, 30] In nature, brown rot fungi are more effective in decomposing cellulose and hemicelluloses like components, whereas, white rot fungi are able to degrade phenol containing structures, whereas, keratin-associated keratinous components can act as a potential feed source for those naturally occurring microorganisms. Furthermore, in later stages of the degradation process the surface wearing off/down or aggregation of the composite occurred due to the further uptake of moisture (H_2O) contents and finally, the polymer molecular chains degrade, followed by transformation to water and CO_2 after a long degradation time. In this background, the possible degradation steps of present phenol grafted keratin-EC based bio-composite are shown by a schematic diagram in Figure 8.

Please insert Fig. 7 here

Figure 7 Biodegradability of keratin-EC (⬚), 15CA-*g*-keratin-EC (⊞), 15GA-*g*-keratin-EC (▨), 10HBA-*g*-keratin-EC (▩) and 20T-*g*-keratin-EC (■) bio-composites buried for prescribed periods: (A) 7 days; (B) 14 days; (C) 21 days; (D) 28 days; (E) 35 days and (F) 42 days (n=3).

Please insert Fig. 8 here

Figure 8 A schematic representation of proposed mechanism of soil burial degradation cycle.

Conclusions

Green chemistry approach toward the synthesis of bio-composites with novel characteristics through enzymatic grafting has several advantages such as: (i) maximal added-value; (ii) eco-friendly processing; (iii) methods which are convenient; (iv) minimum use of water and energy, and finally (v) the methods which only require no or minimal amount of harsh chemicals. In this study, we have developed a self-defensive concept for bacteria-responsive keratin-EC based natural materials that do not cope with such bacterial attacks under their native forms. Therefore, natural phenols were used as functional entities for the preparation of fully bio-based composites. Since reactive reagents are not required for laccase-assisted approach, therefore, the safety concerns are considerably lessened, and simpler manufacturing facilities could be envisioned. Thus, we believe laccase-catalysed grafting of natural phenols onto the previously developed keratin-EC material may provide a “green” alternative to developing bio-composites with novel characteristics.

Acknowledgements

This work was supported by the Cavendish Research Scholarship program of the University of Westminster, a specialised Doctoral Program for the University of Westminster Scholars. On providing the financial support and laboratory facilities for this study, the University of Westminster is thankfully acknowledged.

Notes and references

[a] *Applied Biotechnology Research Group, Department of Life Sciences, Faculty of Science and Technology, University of Westminster, London W1W 6UW, United Kingdom.*

** Corresponding author Tel. +44 020 79115030; fax. +44 020 79115087*

E-mail addresses: hafiz.iqbal@my.westminster.ac.uk (Hafiz M. N. Iqbal) and t.keshavarz@westminster.ac.uk (T. Keshavarz).

[b] *Aix Marseille Université, CNRS, Centrale Marseille, iSm2 UMR 7313, 13397, Marseille, France.*

[1] P. T. Anastas, J. B. Zimmerman, *Environ. Sci. Technol.*, 2003, **37**, 94A.

[2] H. M. N. Iqbal, G. Kyazze, T. Tron, and T. Keshavarz, *Polym. Chem.*, 2014, **5**, 7004.
[3] H. M. N. Iqbal, G. Kyazze, T. Tron, and T. Keshavarz, *Cellulose* 2014, **21**, 3613.
[4] H. M. N. Iqbal, G. Kyazze, T. Tron, and T. Keshavarz, *Carbohydr Polym.*, 2014, **113**, 131.
[5] H. M. N. Iqbal, G. Kyazze, T. Tron, and T. Keshavarz, *Macromol. Mater. Eng.*, 2015, In-Press, DOI: 10.1002/mame.201500003.
[6] A. Aljawish, I. Chevalot, B. Piffaut, C. Rondeau-Mouro, M. Girardin, J. Jasniewski, L. Muniglia, *Carbohydr. Polym.*, 2012, **87**, 537.
[7] N. M. Alves, J. F. Mano, *Int. J. Biol. Macromol.*, 2008, **43**, 401.
[8] A. Brandelli, L. Sala, S. J. Kalil, *Food Research Int.*, 2015, In-Press: doi:10.1016/j.foodres.2015.01.015.
[9] S. Riva, *Trends Biotechnol.*, 2006, **24**, 219.
[10] G. S. Nyanhongo, T. Kudanga, E. N. Prasetyo, G. M. Guebitz, *Biotechnol. Genet. Eng. Rev.*, 2010, **27**, 305.
[11] T. D. Michl, K. E. S. Locock, N. E. Stevens, J. D. Hayball, K. Vasilev, A. Postma, Y. Qu, A. Traven, M. Haeussler, L. Meagher and H. J. Griesserd, *Polym. Chem.*, 2014, **5**, 5813.
[12] Z. Lu, X. Zhang, Z. Li, Z. Wu, J. Song, and C. Li, *Polym. Chem.*, 2015, **6**, 772.
[13] L. Wang, S. He, X. Wu, S. Liang, Z. Mu, J. Wei, F. Deng, Y. Deng, and S. Wei, *Biomaterials* 2014, **35**, 6758.
[14] A. Rukmani, M. Sundrarajan, *J. Ind. Text.*, 2012, **42**, 132.
[15] S. Shahidi, N. Aslan, M. Ghoranneviss, and M. Korachi, *Cellulose* 2014, **21**, 1933.
[16] A. Ultee, M. H. J. Bennik, and R. Moezelaar, *Appl. Environ. Microbiol.*, 2002, **68**, 1561.
[17] M. A. Khosa, A. Ullah, *J. Food Proc. Beverag.*, 2013, **1**, 8.
[18] T. Tanabe, N. Okitsu, A. Tachibana, K. Yamauchi, *Biomaterials* 2002, **23**, 817.
[19] A. Aluigi, C. Vineis, A. Varesano, G. Mazzuchetti, F. Ferrero, C. Tonin, *Eur. Polym. J.*, 2008, **44**, 2465.
[20] A. Prashar, I. C. Locke, C. S. Evans, *Cell Proliferat.*, 2004, **37**, 221.
[21] A. Wattanakornsiri, K. Pachana, S. Kaewpirom, M. Traina, and C. Migliaresi, *J. Polym. Environ.*, 2012, **20**, 801.
[22] A. Vasconcelos, G. Freddi, A. Cavaco-Paulo, *Biomacromolecules* 2008, **9**, 1299.
[23] S. W. Ha, A. E. Tonelli, S. M. Hudson, *Biomacromolecules* 2005, **6**, 1722.
[24] A. Bhattacharya, B. N. Misra, *Prog. Polym. Sci.*, 2004, **29**, 767.
[25] T. Sun, P. Xu, Q. Liu, J. Xue, and W. Xie, *European Polym. J.*, 2003, **39**, 189.
[26] H. N. H. Veras, F. F. G. Rodrigues, and A. V. Colares, *Fitoterapia* 2012, **83**, 508.
[27] G. Milovanovic, M. Stamenic, and D. Markovic, *J. Supercrit. Fluid.*, 2013, **84**, 173.
[28] G. Elegir, A. Kindl, P. Sadocci, and M. Orlandi, 2008, *Enzyme Microb. Technol.*, **43**, 84.
[29] A. C. Vieira, J. C. Vieira, and J. M. Ferra, *J. Mech. Behav. Biomed. Mater.*, 2011, **4**, 451.
[30] W. L. Tham, Z. A. Mohd Ishak, and W. S. Chow, *Polym. Plast. Technol. Eng.*, 2014, **53**, 472.

Cite this: DOI: 10.1039/c0xx00000x

www.rsc.org/xxxxxx

PAPER

List of Figures

Figure 1

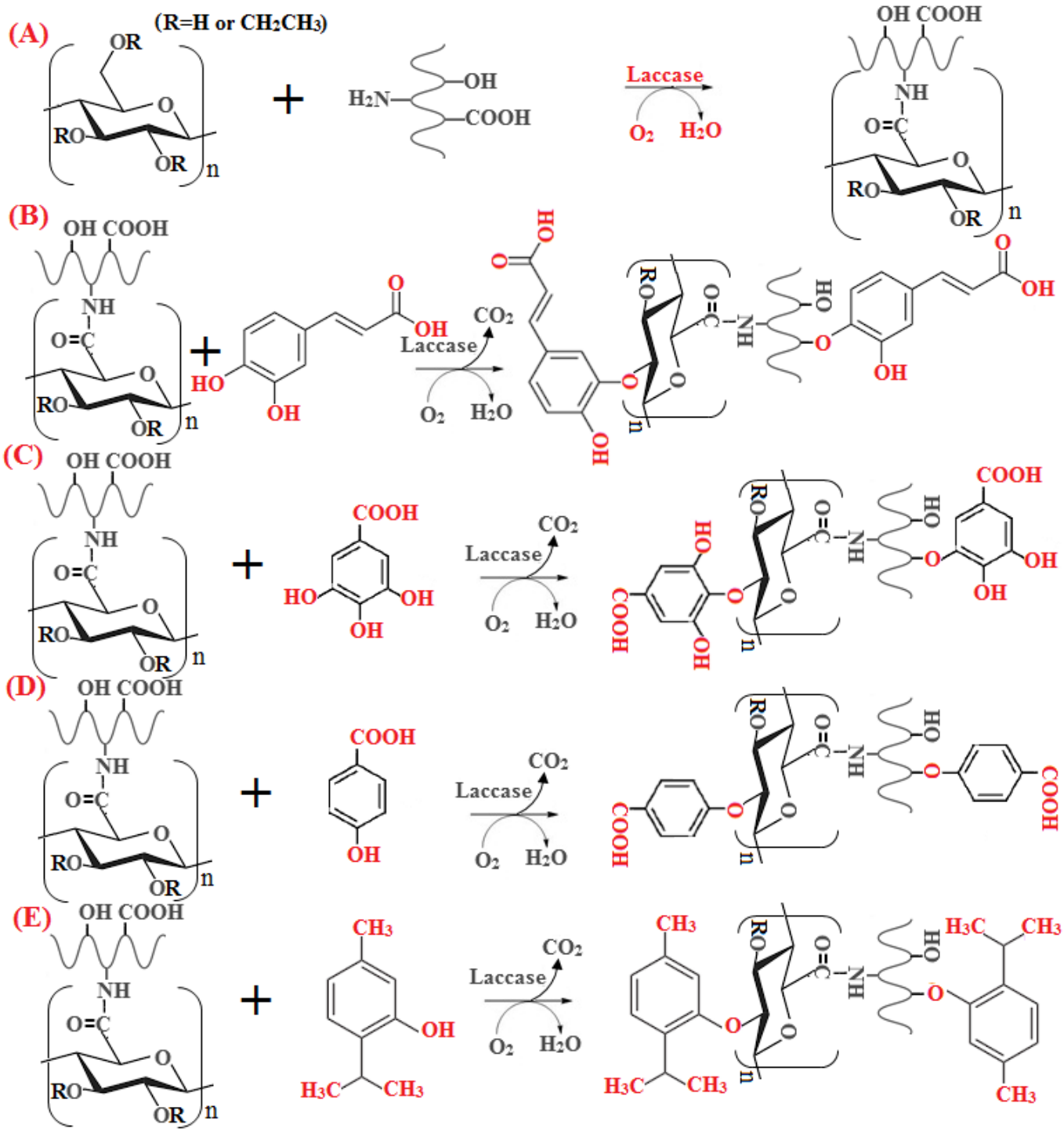

Figure 2

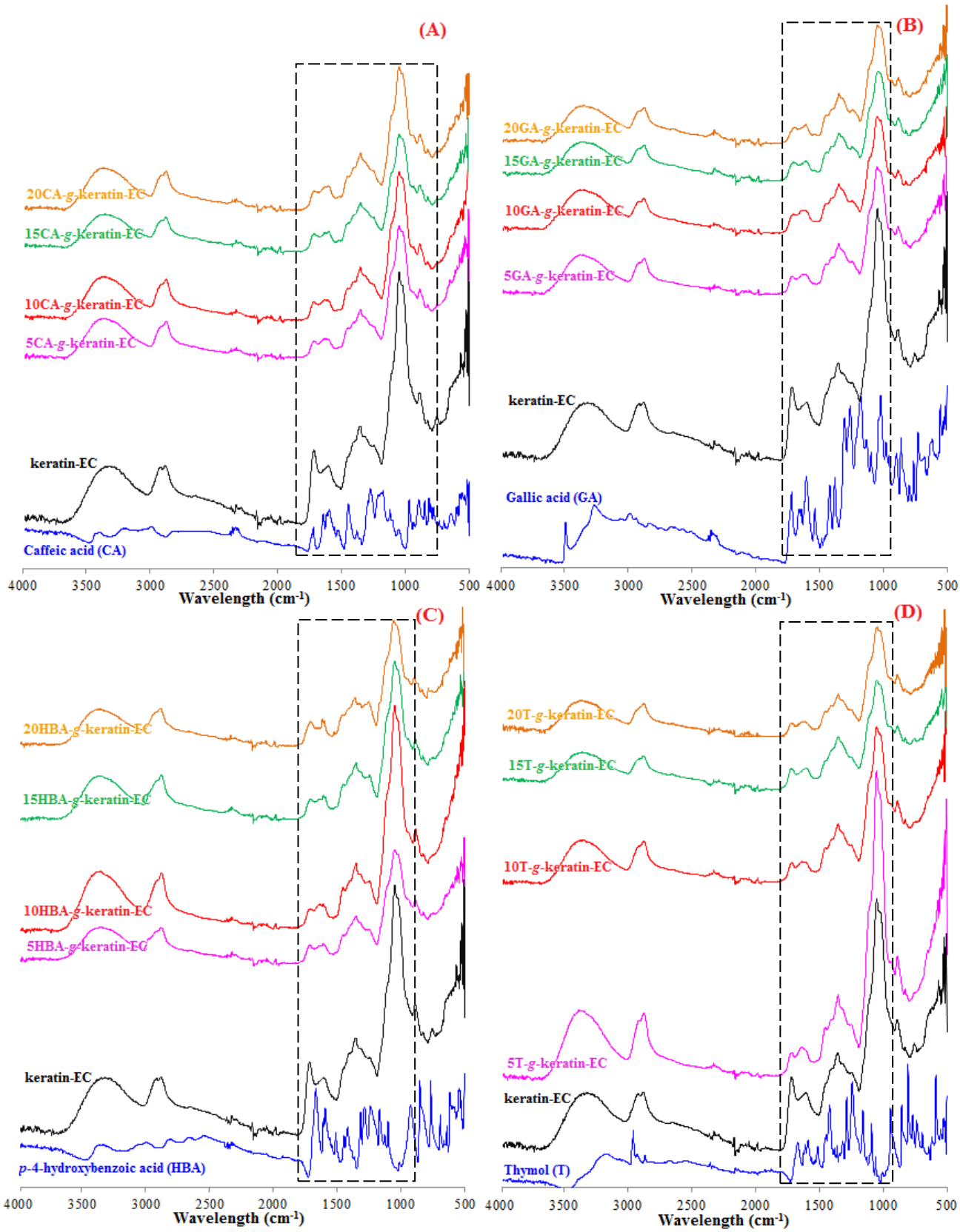
(A)
20CA-g-keratin-EC
15CA-g-keratin-EC
10CA-g-keratin-EC
5CA-g-keratin-EC
keratin-EC
Caffeic acid (CA)
4000 3500 3000 2500 2000 1500 1000 500
Wavelength (cm-1)
(B)
20GA-g-keratin-EC
15GA-g-keratin-EC
10GA-g-keratin-EC
5GA-g-keratin-EC
keratin-EC
Gallic acid (GA)
4000 3500 3000 2500 2000 1500 1000 500
Wavelength (cm-1)
(C)
20HBA-g-keratin-EC
15HBA-g-keratin-EC
10HBA-g-keratin-EC
5HBA-g-keratin-EC
keratin-EC
p-4-hydroxybenzoic acid (HBA)
4000 3500 3000 2500 2000 1500 1000 500
Wavelength (cm-1)
(D)
20T-g-keratin-EC
15T-g-keratin-EC
10T-g-keratin-EC
5T-g-keratin-EC
keratin-EC
Thymol (T)
4000 3500 3000 2500 2000 1500 1000 500
Wavelength (cm-1)

Figure 3

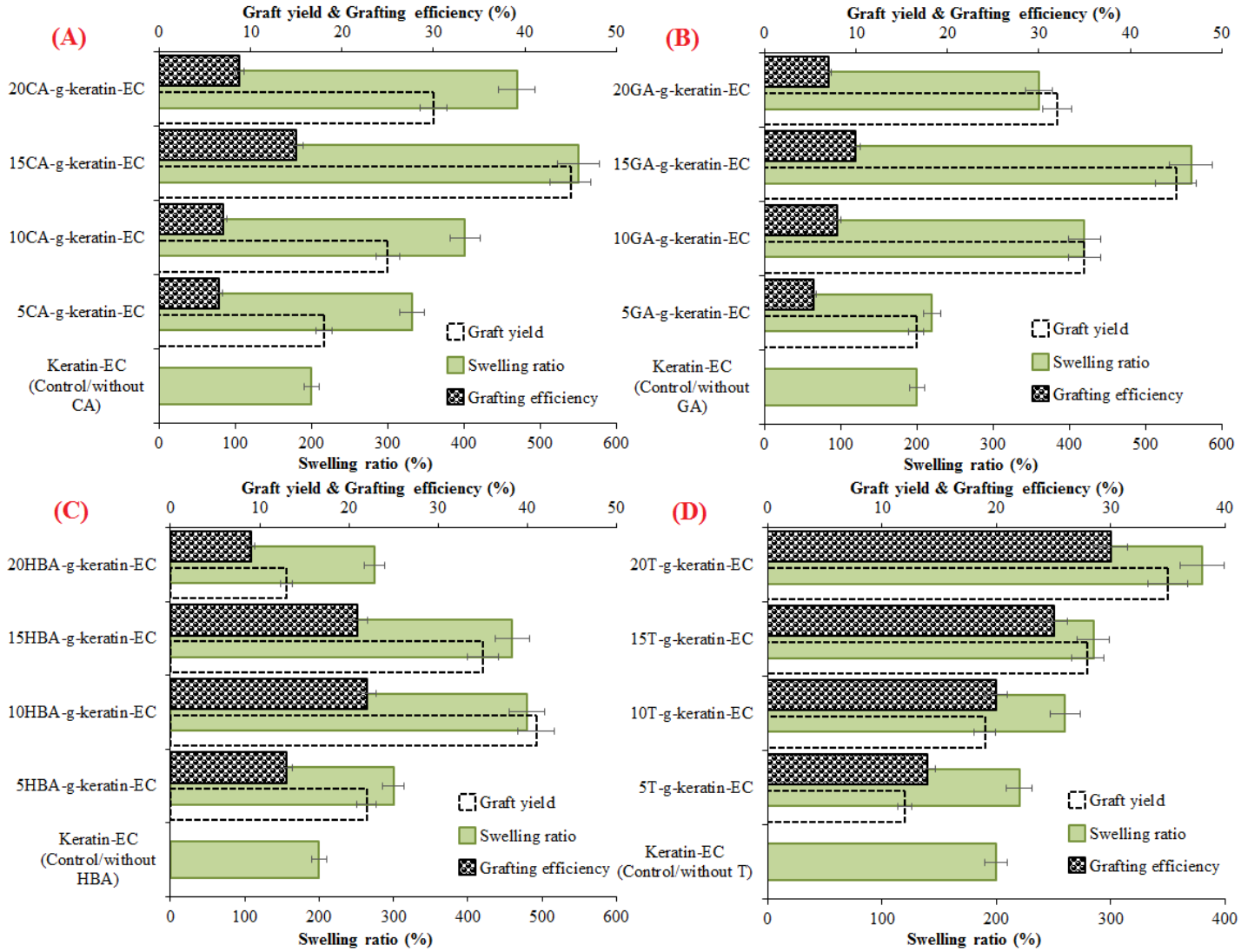

Figure 4

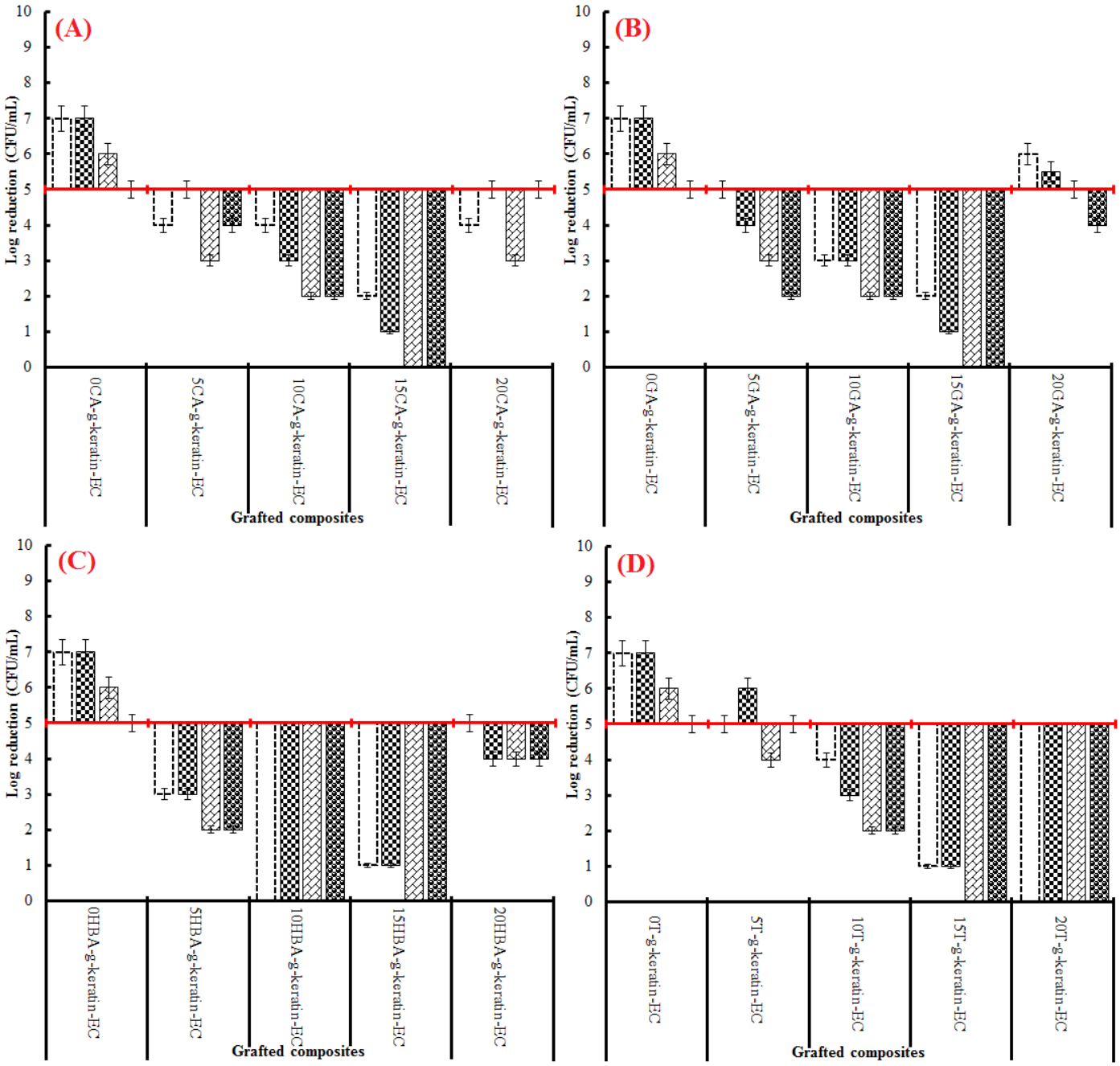
(A)
Log reduction (CFU/mL)
0CA-g-keratin-EC
5CA-g-keratin-EC
10CA-g-keratin-EC
15CA-g-keratin-EC
20CA-g-keratin-EC
Grafted composites
(B)
Log reduction (CFU/mL)
0GA-g-keratin-EC
5GA-g-keratin-EC
10GA-g-keratin-EC
15GA-g-keratin-EC
20GA-g-keratin-EC
Grafted composites
(C)
Log reduction (CFU/mL)
0HBA-g-keratin-EC
5HBA-g-keratin-EC
10HBA-g-keratin-EC
15HBA-g-keratin-EC
20HBA-g-keratin-EC
Grafted composites
(D)
Log reduction (CFU/mL)
0T-g-keratin-EC
5T-g-keratin-EC
10T-g-keratin-EC
15T-g-keratin-EC
20T-g-keratin-EC
Grafted composites

Figure 5

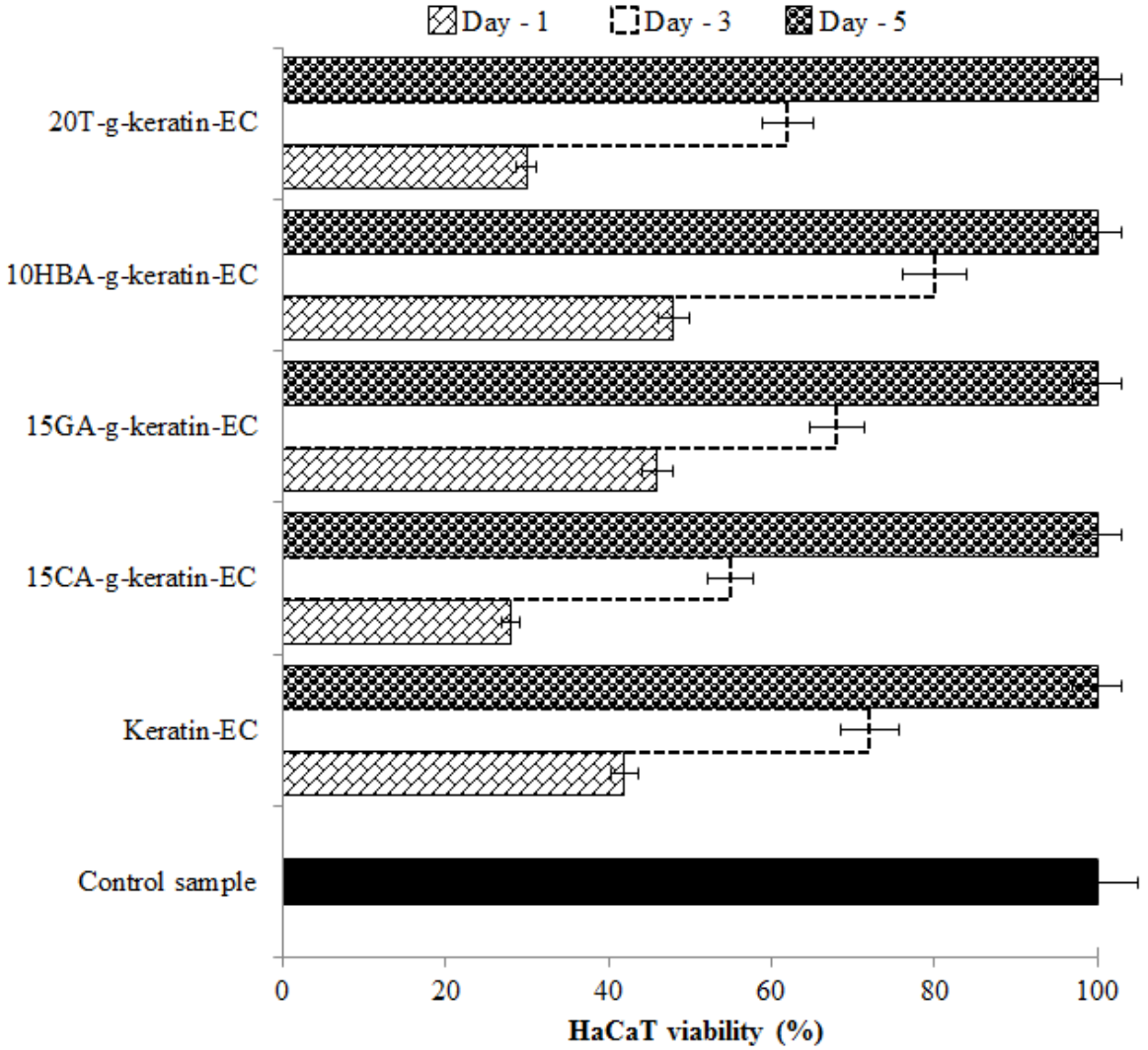

Figure 6

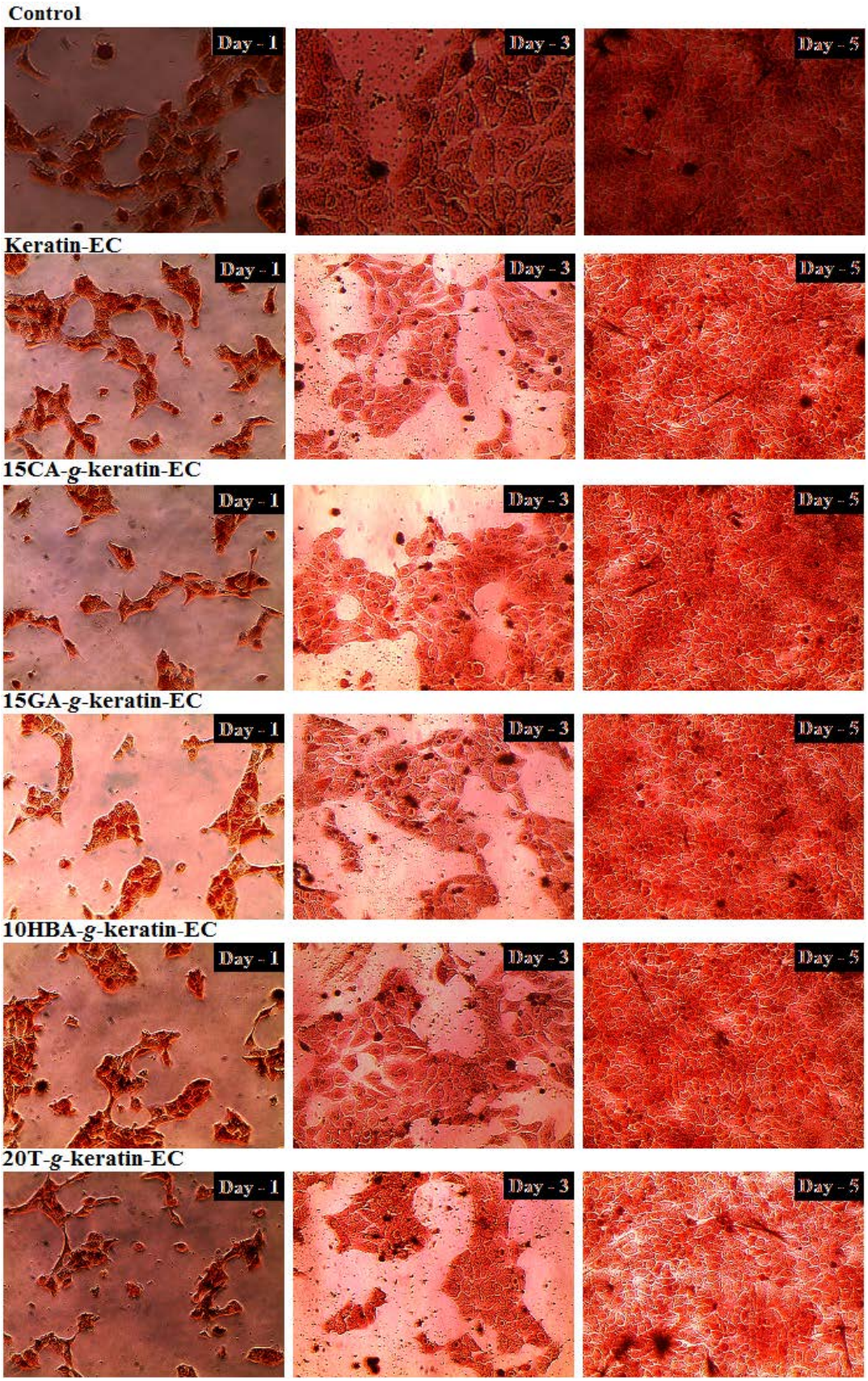
Control
Day - 1
Day - 3
Day - 5
Keratin-EC
Day - 1
Day - 3
Day - 5
15CA-g-keratin-EC
Day - 1
Day - 3
Day - 5
15GA-g-keratin-EC
Day - 1
Day - 3
Day - 5
10HBA-g-keratin-EC
Day - 1
Day - 3
Day - 5
20T-g-keratin-EC
Day - 1
Day - 3
Day - 5

Figure 7

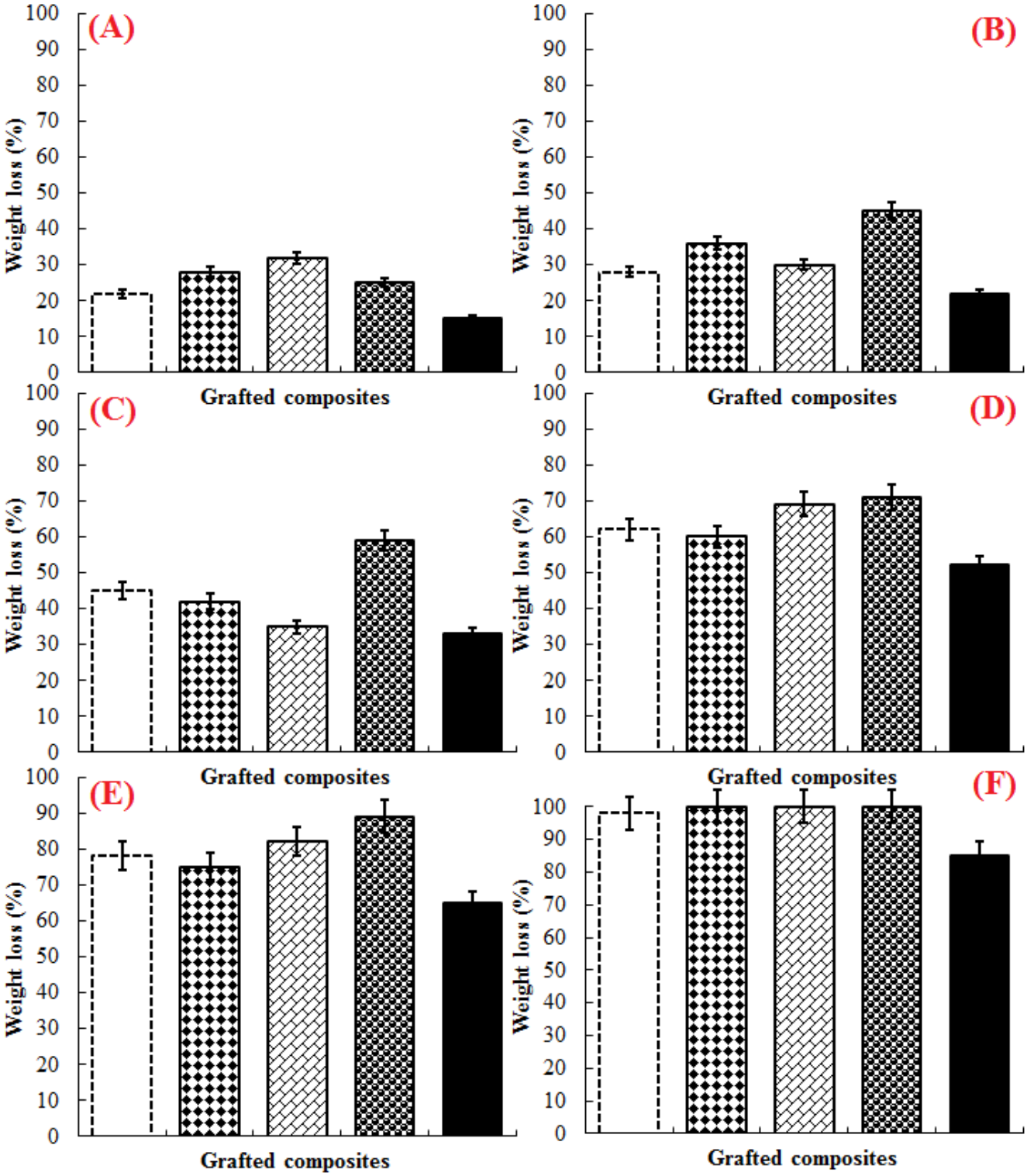

Figure 8

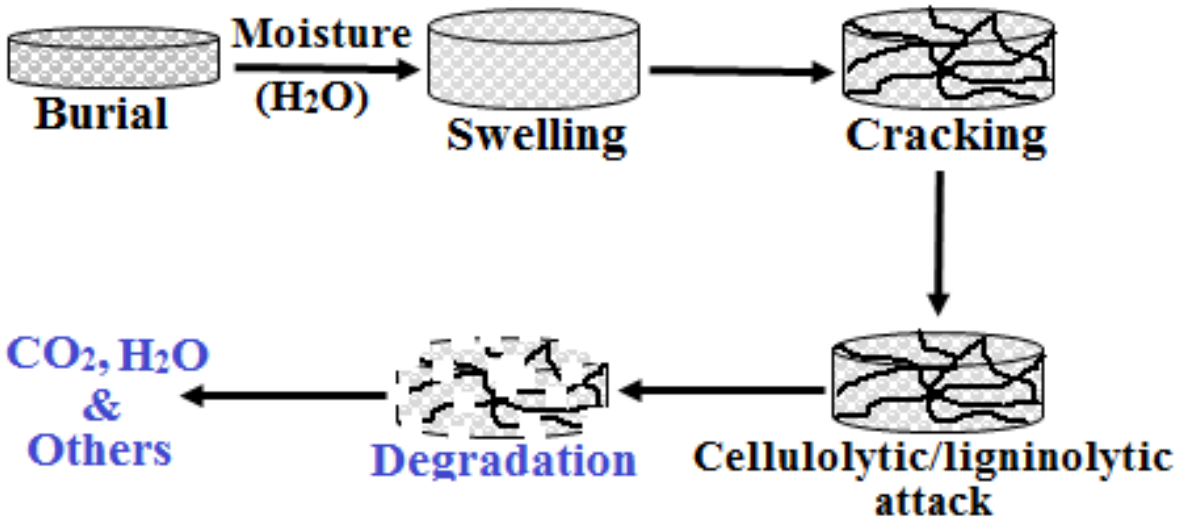
Burial
Moisture
(H2O)
Swelling
Cracking
Cellulolytic/ligninolytic
attack
Degradation
CO2, H2O
&
Others

List of Tables

Table 1 Designation of IDs to the newly synthesised phenol grafted keratin-EC bio-composites subject to the concentration of the phenol used for grafting purposes.

Phenolic component	Concentration (mM)	Composite ID
CA	05	5CA-*g*-keratin-EC
CA	10	10CA-*g*-keratin-EC
CA	15	15CA-*g*-keratin-EC
CA	20	20CA-*g*-keratin-EC
GA	05	5GA-*g*-keratin-EC
GA	10	10GA-*g*-keratin-EC
GA	15	15GA-*g*-keratin-EC
GA	20	20GA-*g*-keratin-EC
HBA	05	5HBA-*g*-keratin-EC
HBA	10	10HBA-*g*-keratin-EC
HBA	15	15HBA-*g*-keratin-EC
HBA	20	20HBA-*g*-keratin-EC
T	05	5T-*g*-keratin-EC
T	10	10T-*g*-keratin-EC
T	15	15T-*g*-keratin-EC
T	20	20T-*g*-keratin-EC